Europe PMC Funders Group
Author Manuscript
*Dev Cell*. Author manuscript; available in PMC 2014 May 08.

Published in final edited form as:
*Dev Cell*. 2013 June 24; 25(6): 599–609. doi:10.1016/j.devcel.2013.05.013.

# Individual Oligodendrocytes Have Only a Few Hours in which to Generate New Myelin Sheaths In Vivo

**Tim Czopka**[1,2,3], **Charles ffrench-Constant**[1,3], and **David A. Lyons**[1,2,*]

[1]Centre for Neuroregeneration University of Edinburgh, Edinburgh EH16 4SB, UK

[2]MS Society Centre for Translational Research University of Edinburgh, Edinburgh EH16 4SB, UK

[3]MRC Centre for Regenerative Medicine, University of Edinburgh, Edinburgh EH16 4UU, UK

## SUMMARY

The number of myelin sheaths made by individual oligodendrocytes regulates the extent of myelination, which profoundly affects central nervous system function. It remains unknown when, during their life, individual oligodendrocytes can regulate myelin sheath number in vivo. We show, using live imaging in zebrafish, that oligodendrocytes make new myelin sheaths during a period of just 5 hr, with regulation of sheath number after this time limited to occasional retractions. We also show that activation and reduction of Fyn kinase in oligodendrocytes increases and decreases sheath number per cell, respectively. Interestingly, these oligodendrocytes also generate their new myelin sheaths within the same period, despite having vastly different extents of myelination. Our data demonstrate a restricted time window relative to the lifetime of the individual oligodendrocyte, during which myelin sheath formation occurs and the number of sheaths is determined.

## INTRODUCTION

Myelinated axons constitute half the volume of the human brain, and myelin has well-established roles in accelerating action potential propagation, maintaining axonal health, and providing nutritional support to associated axons (Fünfschilling et al., 2012; Lee et al., 2012; Nave, 2010; Sherman and Brophy, 2005). Myelination is an ongoing process that commences around birth and continues into at least the third decade in humans (Miller et al., 2012) and one that profoundly affects complex nervous system function during development, adult life, and repair (Franklin and ffrench-Constant, 2008; Liu et al., 2012; Makinodan et al., 2012). The extent of myelination can be regulated by neural activity (Fields, 2010; Wake et al., 2011; Zatorre et al., 2012) and by social isolation of juvenile

©2013 Elsevier Inc.

**LICENSING INFORMATION** This is an open-access article distributed under the terms of the Creative Commons Attribution-NonCommercial-No Derivative Works License, which permits non-commercial use, distribution, and reproduction in any medium, provided the original author and source are credited.

*Correspondence: david.lyons@ed.ac.ukhttp://dx.doi.org/10.1016/j.devcel.2013.05.013.

**SUPPLEMENTAL INFORMATION** Supplemental Information includes three figures and five movies and can be found with this article online at http://dx.doi.org/10.1016/j.devcel.2013.05.013.

Europe PMC Funders Author Manuscripts
Europe PMC Funders Author Manuscripts

Europe PMC Funders Author Manuscripts

Europe PMC Funders Author Manuscripts

mice, which causes a reduction in myelin sheath number per oligodendrocyte and correlates with poor performance in learning and memory tasks (Makinodan et al., 2012). Taken together with the recent evidence for the addition of new myelin sheaths and possible turnover of existing sheaths occurring along already myelinated axons in the adult (Young et al., 2013), these results emphasize that the number of myelin sheaths made by an individual oligodendrocyte is one key parameter by which the extent of myelination is regulated.

Although new oligodendrocytes can be formed throughout life and generate new myelin (Kang et al., 2010; Young et al., 2013), it is also clear that the half-life of myelin protein is very long and that individual myelinating oligodendrocytes can persist throughout life (Savas et al., 2012). Therefore, it has remained unclear as to how individual oligodendrocytes contribute to changes in the number of myelin sheaths made over time in vivo. We do know that individual myelinating oligodendrocytes are plastic, in that they can generate very different numbers of myelin sheaths according to changes in their cellular environment. For example, the presence of supernumerary large caliber axons in the central nervous system (CNS) induces individual oligodendrocytes to generate extra myelin sheaths in vivo (Almeida et al., 2011). In cell culture, it has been shown that oligodendrocytes plated at high density make fewer sheaths per cell compared to those plated at lower densities (Chong et al., 2012). However, what is not known is when individual oligodendrocytes can regulate myelin sheath number during their lifetime. Two fundamentally different modes of myelin sheath production and regulation can be proposed. One possibility is that individual oligodendrocytes only regulate myelin sheath number during a short period when they first generate their myelin sheaths. Alternatively, mature oligodendrocytes might be capable of regulating myelin sheath number at any time. If the former is true, this would indicate that there is a restricted period of plasticity in the regulation of myelin sheath number by individual oligodendrocytes and that new myelin made at distinct periods of life would necessitate the differentiation of new oligodendrocytes. If the latter is true, it would indicate that individual oligodendrocytes can remain responsive to environmental cues longer term and thus contribute to the formation of new myelin as well as the regulation of myelin turnover.

Here, we used live imaging and manipulation of Fyn kinase function in zebrafish to study the dynamic regulation of myelin sheath number by individual oligodendrocytes in vivo. We show that although global myelination in the zebrafish spinal cord continues over time, each individual oligodendrocyte only makes new myelin sheaths during a very short and highly dynamic period of about 5 hr following initiation of myelination. This short period of myelin sheath generation is consistent, regardless of the final extent of myelination of the cell. We also observed that myelin sheath number is regulated by a low level of retraction over the following two days of maturation and that after this time the myelin sheath repertoire of individual oligodendrocytes remains remarkably stable. These data provide critical insight as to how the plasticity of myelination is regulated by individual cells.

## RESULTS

It is well known that CNS myelination is an ongoing process. Here, we use the relatively simple system of the larval zebrafish spinal cord to study how single oligodendrocytes

Europe PMC Funders Author Manuscripts

Europe PMC Funders Author Manuscripts

contribute to the dynamic regulation of myelination over time. We first show that between 4 and 8 days postfertilization (dpf) there is a significant increase in myelin sheath number and myelinated axon number in the zebrafish spinal cord as assessed by Tg(mbp:EGFP-CAAX), which labels all myelin sheaths (Figure 1A) (Almeida et al., 2011). We confirm previous data that at the global level, myelination in the spinal cord occurs not only in a temporal gradient but also in a striking spatial gradient from anterior to posterior (Figure 1A). We further show that there is a corresponding increase in myelinating oligodendrocyte number over this period and also according to an anterior-posterior gradient, as assessed by Tg(mbp:EGFP) (anterior spinal cord, 4 dpf 65 ± 11, 8 dpf 101 ± 16, $p < 0.0001$; posterior spinal cord, 4 dpf 17 ± 5, 8 dpf 46 ± 6, $p < 0.0001$ ($n = 10$ for all) (Figures 1B and 1C). Interestingly, when we characterized the timing of myelination along individual axons (labeled with a reporter of mature neurons and axons, cntn1b:mCherry, together with Tg(mbp:EGFP-CAAX)), we saw that single axons were increasingly myelinated along their length over time (Figures 1D and 1E), as predicted by previous EM data in cat (Remahl and Hildebrand, 1990). The increase in myelination along the length of axons was accomplished by both the longitudinal growth of individual myelin sheaths and also by the addition of new myelin sheaths to the same axon at different times (Figures 1D–1G). These data indicate that newly differentiating oligodendrocytes contribute to the new myelin generated over time, but it remains unclear if already existing myelinating oligodendrocytes contribute to the global increase in myelination.

In order to characterize when individual oligodendrocytes generate their myelin sheaths in vivo, we carried out time course and time-lapse imaging of fluorescent transgenic reporters in the embryonic and larval zebrafish spinal cord. Examination of the transgenic reporters Tg(nkx2.2a:meGFP) (which labels oligodendrocytes (Kirby et al., 2006) and Tg(cntn1b:mCherry) demonstrated that Tg(nkx2.2a:meGFP) could be used to visualize oligodendrocytes and their nascent myelin sheaths during the initiation of myelination in the living spinal cord (Figures 2A–2C). Time-lapse analyses of nkx2.2a:meGFP-expressing oligodendrocytes allowed observation of the transformation of exploratory processes into nascent myelin sheaths within a few hours (Figure 2D) and also showed that nascent myelin sheaths are occasionally retracted over the same time (Figure 2E).

Having established that we could observe the behavior of oligodendrocytes and their myelinating processes, we monitored the formation of all new myelin sheaths by individual oligodendrocytes from the initiation of myelination through to their establishment of a stable number of sheaths (Figures 2F and 2G; Movie S1 available online). Analyses of Tg(nkx2.2a:meGFP) at 3 dpf revealed a gradient in oligodendrocyte maturation (as predicted by the known gradient in myelination seen at 4 dpf, Figure 1), with oligodendrocytes of myelinating morphology generally located more anterior relative to those with a premyelinating morphology (Figure 2A). Therefore, in order to standardize our characterization of the initiation of myelination by individual oligodendrocytes, we defined a time point zero for each individual oligodendrocyte as the time at which it formed its first myelin sheath (Figures 2F and 2G). Regardless of where we looked along the length of the spinal cord, or precisely when we started our analyses, we saw that each individual oligodendrocyte initiated formation of its final new myelin sheath within an average of 5 hr (263 ± 80 min, 16 cells in 11 animals) of having formed its first myelin sheath (Figures 2F

Europe PMC Funders Author Manuscripts

Europe PMC Funders Author Manuscripts

and 2G). During this time window, we also observed retraction of nascent myelin sheaths (Figures 2F and 2G), although the majority (80% ± 13%) of nascent myelin sheaths were maintained throughout our analyses, suggesting that the mechanisms that determine which axons are to be myelinated are largely determined prior to formation of nascent myelin sheaths.

The lack of any observed increase in myelin sheath number by individual oligodendrocytes after the initial 5 hr period of initiation of myelination using our time-lapse analyses, when global myelination is proceeding, suggests that new myelin sheaths generated over this period must be made by newly differentiating oligodendrocytes. In order to test whether individual mature oligodendrocytes make new myelin sheaths over a longer period of time, we followed 20 additional cells from 4 dpf (i.e., the end of our time-lapse analyses) up to 20 dpf (Figure 3). We saw that none of these 20 cells ever made a new myelin sheath, even though global myelination in the spinal cord continues throughout this time. Eleven of these 20 cells showed absolutely no change in myelin sheath number, three cells removed a single myelin sheath, two removed two, three removed three, and one oligodendrocyte retracted six myelin sheaths (Figure 3B). The overall proportion of such retractions was only 8% of the total number of myelin sheaths (22/273) in the cells analyzed. A more careful breakdown of the timing of these 22 retractions showed that the vast majority (19/22) occurred within the first 2 days of maturation (Figure 3C). These data, in combination with our time-lapse analyses, show that myelin sheath formation occurs rapidly within the first few hours following initiation of myelination and that a period of limited myelin sheath retraction of about 2 days follows, after which time oligodendrocyte morphology and myelin sheath number remain very stable. Furthermore, when myelin sheaths were retracted by mature oligodendrocytes, the complete retraction of these sheaths and the proximal process could take several days (Figure 3D), in contrast to the rapid events during initiation of myelination. Therefore, these observations show that the dynamic behavior of individual oligodendrocytes changes dramatically following the short period of new myelin sheath formation.

To test further whether the generation of new myelin sheaths by individual cells is restricted to this period of only a few hours in the life of the oligodendrocyte, we sought to identify manipulations capable of increasing and decreasing myelin sheath number per cell. Previous studies have implicated Fyn kinase as a downstream integrator of axo-glial signals in oligodendrocytes that controls myelination (Krämer-Albers and White, 2011; Laursen et al., 2009; Umemori et al., 1994; Wake et al., 2011), and we reasoned that one way in which Fyn might affect myeli-nation in vivo is by regulating the number of myelin sheaths made by individual cells. Fyn activity is regulated through phosphorylation of a C-terminal Tyrosine, whereby dephosphorylation results in kinase activation (Krämer-Albers and White, 2011; Laursen et al., 2009), allowing us to generate a transgenic line with constitutively active Fyn in all myelinating oligodendrocytes Tg(mbp:ca-Fyn) (Figure S1). Importantly, by using myelin basic protein upstream regulatory sequence, which drives gene expression following onset of terminal differentiation, but prior to the establishment of nascent myelin sheaths (Figure S1), we were able to activate Fyn kinase function immediately prior to the initiation of myelination. By analyzing single cell morphology in such animals, we observed a 33% increase in myelin sheath number per oligodendrocyte in Tg(mbp:ca-Fyn) animals (wild-

Europe PMC Funders Author Manuscripts

Europe PMC Funders Author Manuscripts

type, 15 ± 4, 33 cells; Tg(mbp:wt-Fyn), 15 ± 5, 32 cells; Tg(mbp:ca-Fyn), 20 ± 6, 36 cells, $p < 0.01$) (Figures 4A and 4B). This increase in sheath number per cell occurred without any change in oligodendrocyte number (Figures 5A–5C) or myelin sheath length (Figure 4C), indicating that more axonal space was myelinated in Tg(mbp:ca-Fyn) animals. In order to test this directly, we analyzed individual axons in wild-type and Tg(mbp:ca-Fyn) animals and found that individual myelinated axons in Tg(mbp:ca-Fyn) were covered by about 69% more myelin along their length compared to controls by 5 dpf (wild-type 35% ± 20%, 13 axons in nine animals; Tg(mbp:ca-Fyn) 59% ± 25, ten axons in ten animals; $p = 0.016$) (Figure 5D). We also carried out transmission electron microscopy at 8 dpf and observed a 21% increase in myelinated axon number in Tg(mbp:ca-Fyn) animals (wild-type 80 ± 10, four animals, Tg(mbp:ca-Fyn) 97 ± 7, five animals, $p = 0.02$) (Figures 5F and 5G). Furthermore, we saw that there was no change in the range of axons myelinated (with respect to caliber or general distribution in the spinal cord) and instead that Tg(mbp:ca-Fyn) animals had a larger proportion of myelinated axons with a perimeter greater than 1.5 μm (0.5 μm diameter) (Figure 5H). We saw a corresponding decrease in the number of such larger caliber that were unmyelinated in Tg(mbp:ca-Fyn) animals (wild-type 41% ± 19%; Tg(mbp:ca-Fyn) 18% ± 6%, $p = 0.04$) (Figures 5H and 5I). Together, these data suggest that mbp:ca-Fyn-expressing oligodendrocytes more efficiently myelinate the axons that are competent for myelination at these stages.

To test whether disruption of Fyn kinase signaling caused a decrease in myelin sheath generation by oligodendrocytes, we took a previously validated Morpholino-based approach (Jopling and den Hertog, 2005) and observed a reduction in myelination, without any obvious defects in general development (Figure S2). Analyses of single oligodendrocyte morphology showed that *fyn* morphant oligodendrocytes made 36% fewer myelin sheaths than their wild-type counterparts at 4 dpf (wild-type 14 ± 5, 37 cells; *fyn* MO 9 ± 4, 34 cells, $p < 0.001$), also without any change in average sheath length (Figures 4D–4F). This shows that Fyn is essential for formation of the normal number of myelin sheaths per oligodendrocyte.

Having confirmed that manipulation of Fyn signaling could increase or decrease the number of sheaths formed by individual oligodendrocytes, we carried out time-lapse analyses of 13 individual oligodendrocytes in 11 *fyn* morphants and 14 oligodendrocytes in ten Tg(mbp:ca-Fyn) animals to see if sheath formation occurred during the same short dynamic period as in wild-type (Figure 6; Movies S2 and S3). As expected, oligodendrocytes in Tg(mbp:ca-Fyn) animals made more total ensheathments than oligodendrocytes in *fyn* morphants and wild-types (wild-type 13 ± 4, *fyn* MO 9 ± 3 [$p < 0.01$], Tg(mbp:ca-Fyn) 20 ± 6 [$p < 0.001$]), but the small number of retractions appeared the same in each condition over the course of the analyses (Figures 6A–6E). Strikingly, however, these time-lapse studies revealed that the individual oligodendrocytes in *fyn* morphant and Tg(mbp:ca-Fyn) animals also generated their myelin sheaths within 5 hr of having formed their first nascent sheath (*fyn* MO, 208 ± 74 min; Tg(mbp:ca-Fyn) 261 ± 83 min, Figures 6A–6D and 6F; Movies S2 and S3), despite the fact that oligodendrocytes in Tg(mbp:ca-Fyn) animals made over 2-fold more ensheathments than in *fyn* morphants (Figure 6E). Furthermore, the average length of the period of new myelin sheath production in Tg(mbp:ca-Fyn) animals (261 ± 83 min) was

almost identical to that observed in wild-type (263 ± 80 min), despite the difference in their relative extent of myelination.

## DISCUSSION

Together, our data show that oligodendrocytes generate new myelin sheaths only during a remarkably short and dynamic time window of about 5 hr of their life in vivo. This synchronous formation of myelin sheaths mirrors observations made in a previous coculture experiment, where it was found that oligodendrocytes cultured with retinal ganglion cells also generated their myelin sheaths in a short period (Watkins et al., 2008). Indeed the duration of the period of active myelin sheath generation observed in the in vitro study (about 12 hr) and ours is remarkably similar, given the interspecies and in vivo versus in vitro differences. However, an important contrast to the in vitro study was that we found no evidence of dynamic exploratory processes after oligodendrocytes form their final new myelin sheath. Instead, we observed that, in vivo, oligodendrocyte behavior changed dramatically following initiation of the last new myelin sheath with no further exploratory activity and with sheath retractions at later stages taking place much more slowly than during the rapid initiation of myelination. Our observation of a remarkably consistent period of myelin sheath production that is irrespective of the number of myelin sheaths generated, or the precise time or location of the individual cell, strongly suggests that the duration of the period of myelin sheath production is an intrinsic feature of the oligodendrocyte. Future studies will be required to elucidate the cell and molecular mechanisms that regulate the duration of this period and the dramatic change in cell behavior that follows the end of the initiation phase of myelination.

In addition to characterizing how single oligodendrocytes generate new myelin sheaths over time, our study also provided documentation of myelin sheath retractions by single oligodendrocytes in vivo. The first key point is that the total proportion of retractions is very low compared to the number of ensheathments made, even though only a relatively small number of axons (about 200 out of a total of several thousand) are myelinated in the spinal cord during the time of our analyses. This means that the cell-cell and molecular interactions that regulate which axons are ensheathed and myelinated, and which are not, must be made prior to the ensheathment of the “correct” axons. One possibility is that the retractions observed in our analyses are due to the initial ensheathment of incorrect axons. Preliminary analyses, however, suggest that retractions of individual myelin sheaths are sometimes made from axons that otherwise remain myelinated (Figure S3; Movies S4 and S5), suggesting that this is not the only driving force for myelin sheath retraction. Indeed, recent data suggest that there may be a degree of ongoing myelin sheath turnover throughout life (Young et al., 2013), where individual sheaths would be retracted and replaced over time. Our analyses of the temporal progression of myelin sheath retractions by single oligodendrocytes suggests, however, that the majority of retractions are made within 1–2 days following initiation of myelination, after which time myelin sheath number is remarkably stable. Further extensive studies are required to elucidate the dynamics of myelin sheath retractions later in life and in areas with well-defined turnover of myelin.



Europe PMC Funders Author Manuscripts
Europe PMC Funders Author Manuscripts

Europe PMC Funders Author Manuscripts

Europe PMC Funders Author Manuscripts

For the purposes of this study, we have focused on the ability of single oligodendrocytes to regulate myelin sheath number, which is regulated by environmental cell-cell interactions. Here, we identify Fyn kinase as a putative integrator of the signals that control myelin sheath number in the oligodendrocyte. In addition to myelin sheath generation, there are additional modes by which the extent of myelination can be regulated in vivo. Over-expression of a specific isoform of Neuregulin (Neuregulin 1 type I) can lead to the myelination of axons in the brain that are not normally myelinated (Brinkmann et al., 2008). It has also become clear that the thickness of individual myelin sheaths is another parameter by which the extent of myelination can be regulated in juvenile and adult animals (Brinkmann et al., 2008; Liu et al., 2012; Makinodan et al., 2012). It will be interesting to determine whether the thickness of already established myelin sheaths can be dynamically regulated over time or whether differences in myelin sheath thickness, such as those detected in socially isolated animals, are due to differences in the extent of myelination by newly differentiating oligodendrocytes.

An important implication of our study is that new myelin sheaths made at distinct stages of life must be generated by newly differentiating oligodendrocytes. This is entirely plausible given the lifelong presence of oligodendrocyte precursor cells (OPCs) in mammals and zebrafish (Dawson et al., 2003; Park et al., 2007) that primarily generate new oligodendrocytes in vivo (Kang et al., 2010; Richardson et al., 2011), and the fact that newly differentiating oligodendrocytes contribute to remyelination in adults in vivo (Zawadzka et al., 2010). This in turn identifies a potential bottleneck to efficient repair. If oligodendrocytes have a limited period to remyelinate axons, then unless the axonal environment is fully permissive for remyelination during this period, there will be a limited degree of repair. This is an example of the dysregulation hypothesis proposed to explain remyelination failure in MS (Franklin, 2002).

In summary, our work proposes the existence of a restricted period during the life of the myelinating oligodendrocyte when new myelin sheaths are generated and during which the extent of myelination can be regulated in vivo.

## EXPERIMENTAL PROCEDURES

### Fish Husbandry

The following wild-type, transgenic, and mutant zebrafish lines were used: AB, TL, *golden* (Lamason et al., 2005), *casper* (White et al., 2008), Tg(nkx2.2a: mEGFP) (Kirby et al., 2006; Ng et al., 2005), Tg(sox10(7.2):mRFP) (Kirby et al., 2006), Tg(mbp:EGFP), and Tg(mbp:EGFP-CAAX) (Almeida et al., 2011). For this study, we generated the following transgenic lines: Tg(cntn1b (5kb):mCherry), Tg(mbp:mCherry-2A-wt-Fyn), and Tg(mbp:mCherry-2A-ca-Fyn). Throughout the text and figures, we refer to Tg(mbp:mCherry-2A-wt-Fyn) as Tg(mbp:wt-Fyn) and Tg(mbp:mCherry-2A-ca-Fyn) as Tg(mbp:ca-Fyn) for simplicity. All animals were maintained in accordance with UK Home Office guidelines.

Europe PMC Funders Author Manuscripts

Europe PMC Funders Author Manuscripts

## Plasmid Construction

We cloned a 5 kb DNA fragment upstream of the ATG of the *cntn1b* gene from TL genomic DNA using the following *att* recombination site containing primers: attB4_cntn1b(5kb)F: GGGGACAACTTTGTATAGAAAAGTTGCTGATCATTTGAGTCCAAGCG, attB1R_cntn1b(ATG)R: GGGGACTGCTTTTTTGTACAAACTTGGATCCAGCAGTCCAAAAACC. The PCR product was recombined with pDONR_P4-P1R using BP clonase (Invitrogen) to generate the 5′ element clone p5E_cntn1b(5kb).

We generated a 5′ element clone p5E_sox10 by excising a 7.2 kb sox10 promoter fragment from p7.2sox10:mRFP (Kirby et al., 2006) via XbaI (blunted with Mung Bean Nuclease) and SalI restriction sites. This fragment was ligated into p5E_MCS (Tol2kit), which was opened with HindIII (blunted with Mung Bean Nuclease) and SalI restriction enzymes.

We have previously generated a p5E_mbp (Almeida et al., 2011).

To generate wild-type and constitutively active Fyn transgenic constructs, full-length *fyna* was initially amplified from complementary DNA (cDNA) of the AB strain and cloned in pCRII-Topo. A PTV1-2A (2A) sequence, which is a short linker peptide that induces a peptide strand break during messenger RNA (mRNA) translation to obtain two separate proteins from a single open reading frame (Provost et al., 2007) (Figure S1), was added to the 5′ of the ATG of *fyna* using the following primers: (P2A_fyna_F: GGATCCGGAGCCACGAACTTCTCTCTGTTAAAGCAAGCAGGAGACGTGGAAGA AAACCCCGGTCCTATGGGCTGTGTGCAATGTAAG, fyna_R: TTAGAGGTTGTCCCCGGGTTG). This plasmid served as template to generate a constitutively active variant of Fyn using site-directed mutagenesis (Stratagene). We introduced an A1592T mutation (amino acid exchange Y531F) with the following primers: (Y531F_F: GCCACTGAACCACAGTTCCAACCCGGGGACAACC, Y531F_R: GGTTGTCCCCGGGTTGGAACTGTGGTTCAGTGGC). The 2A-wt-Fyn and 2A-ca-Fyn inserts were then subcloned into pCS2+ (contains a SV40 late pA 3′ of the MCS) using BamHI and XhoI sites. These plasmids were used to generate attB2_2A-wt-Fyn-pA_attB3R and attB2_2A-ca-FynpA_attB3R by PCR amplification using the following primers: (attB2_2A_F: GGGGACAGCTTTCTTGTACAAAGTGGCAGGATCCGGAGCCACGAACTTC, attB3R_pA_R: GGGGACAACTTTGTATAATAAAGTTGAAAAAACCTCCCACACCTCCC). The PCR products were recombined with pDONR_P2-P3R using BP clonase (Invitrogen) to generate the 3′ element clones p3E_2A-wt-fyn-pA and p3E_2A-ca-fyn-pA.

All Tol2 transgenesis constructs were recombined using the abovementioned and other donor clones (all of which are components of the Tol2kit [Kwan et al., 2007]) and pDestTol2CG2 and pDestTol2pA2 using LR clonase II Plus (Invitrogen).

## Microinjection and Generation of Transgenic Zebrafish

Fertilized eggs were injected with 1 nl of 10–20 ng/μl plasmid DNA and 25 ng/μl transposase mRNA. Injected fish were analyzed as mosaics or grown to adulthood to raise

Europe PMC Funders Author Manuscripts

Europe PMC Funders Author Manuscripts

stable transgenic lines. For Fyn loss-of-function experiments, eggs were injected with 2.5 ng of a Morpholino, which targets both zebrafish *fyn* paralogs, *fyna* and *fynb*, to generate a more complete knockdown of Fyn function (Jopling and den Hertog, 2005).

### RNA Extraction and RT-PCR

Total RNA was extracted from zebrafish embryos using the RNeasy Kit (QIAGEN), and cDNA was transcribed using AccuScript reverse transcriptase (Stratagene). Total *fyna* transcripts were amplified with the following primers: fynaF: ATGGGCTGTGTGCAATGTAAG; fynaR: CCTTTCGTGGTCTCACTCTC. The transcript of the *mcherry-2A-fyna* transgene was amplified using mCherry forward and fyna reverse primers (mCherryF: CCTGTCCCCTCAGTTCATGT, fynaR: as above).

### Western Blotting

To test *fyn* Morpholino-mediated knockdown, injected zebrafish embryos were lysed at 3 days postfertilization (dpf) in RIPA buffer. To test self-cleavage and Tyrosine mutation of Fyn transgenic constructs, cultured HEK293T cells were cotransfected with modified Fyn constructs (β-actin:gal4 + uas:egfp-2A-wt-fyn; β-actin:gal4 + uas:mcherry-2A-wt-fyn, β-actin:gal4 + uas:m-cherry-2A-ca-fyn) using Lipofectamine2000 (Invitrogen) and lysed in RIPA buffer 1 day posttransfection. Western blotting was carried out using antibodies against Fyn (Santa Cruz Technologies), EGFP (Invitrogen), phospho-SFK-Y418 and phospho-SFK-Y529 (Invitrogen), GAPDH (Chemicon), beta-actin, and appropriate HRP-conjugated secondary antibodies (all from Amersham). Films were developed using chemi-luminescence.

### Transmission Electron Microscopy

Tissue preparation for transmission electron microscopy (TEM) was carried out as previously described in detail (Czopka and Lyons, 2011). Images were taken with a Phillips CM120 Biotwin. Data analysis was performed using ImageJ.

### Live Imaging and Data Analysis

Embryos were embedded in 1.5% low melting point agarose in embryo medium with Tricaine. All images were taken from lateral views of the spinal cord, anterior being left and dorsal being up. Single time point live imaging was carried out either on a Zeiss LSM 710 or a Zeiss Imager Z1 with an Apotome2 structured illumination unit. Time-lapse imaging was carried out on a Zeiss LSM 710 with a heated stage. For analyses of single oligodendrocyte morphology, we used *golden* and *casper* pigment mutants to allow live imaging at larval stages. We injected plasmid DNA encoding mbp:EFGP-CAAX into *golden* or *casper* eggs at the 1–2 cell stage and typically imaged between one and three cells per animal. For long-term time course imaging beyond 4 dpf, individual animals were mounted once a day in low melting point agarose, imaged, and subsequently released from the agarose and grown and fed as normal. Note that when individual cells were imaged, the corresponding figure panel will be designated as either mbp:EGFP-CAAX or cntn1b:mCherry, whereas when stable transgenic lines are imaged, this will be indicated by the “Tg” designation, e.g., “Tg(mbp:EGFP-CAAX).”

Europe PMC Funders Author Manuscripts

Europe PMC Funders Author Manuscripts

To image the percentage of myelination along the length of individual axons over time, we injected plasmid DNA encoding cntn1b:mCherry into Tg(mbp:EGFP-CAAX) embryos at the 1–2 cell stage and imaged animals from 3 through 9 dpf. We identified single myelinated axons at the first time point each animal was analyzed and assessed the relative change in their myelination over time. The individual axonal stretches analyzed ranged from 70 to 480 μm, and the total axonal distance analyzed was 2.5 mm in wild-type axons (from 13 axons in 9 animals) and 1.8 mm in Tg(mbp:-ca-Fyn) animals (from ten axons in ten animals). Imaging data were documented and analyzed using Zeiss Zen, Axiovision, and ImageJ software. All data are expressed as mean ± SD. For statistical analyses we used Student's two-tailed t test and one- and two-way ANOVA as is indicated in the figure legends.

Statistical significance is indicated as follows: * $p < 0.05$, ** $p < 0.01$, *** $p < 0.001$.

## Supplementary Material

Refer to Web version on PubMed Central for supplementary material.

## Acknowledgments

We thank Carl Tucker, Paul Wright, and Patricia Smart for fishroom support and Chris Jopling for information about the *fyn* MO. We would also like to thank Crerar hotels and Sally Womersley for helping to provide microscopes. A very special thanks goes to our late and great colleague Chi-Bin Chien and the Chien laboratory for the tol2kit and to Len Zon for the *casper* line. We are grateful to Peter Brophy, Ben Emery, Kelly Monk, William Talbot, and members of the Lyons and ffrench-Constant laboratories for critical reading of the manuscript. This work was supported by a David Phillips Fellowship from the BBSRC, a Research Prize from the Lister Institute, and an International Reintegration Grant (to D.A.L.), an EMBO Long-Term Fellowship (to T.C.), and a Wellcome Trust Programme Grant (to C.ff.-C.).

## REFERENCES

Almeida RG, Czopka T, ffrench-Constant C, Lyons DA. Individual axons regulate the myelinating potential of single oligodendrocytes in vivo. Development. 2011; 138:4443–4450. [PubMed: 21880787]

Brinkmann BG, Agarwal A, Sereda MW, Garratt AN, Müller T, Wende H, Stassart RM, Nawaz S, Humml C, Velanac V, et al. Neuregulin-1/ErbB signaling serves distinct functions in myelination of the peripheral and central nervous system. Neuron. 2008; 59:581–595. [PubMed: 18760695]

Chong SYC, Rosenberg SS, Fancy SPJ, Zhao C, Shen Y-AA, Hahn AT, McGee AW, Xu X, Zheng B, Zhang LI, et al. Neurite outgrowth inhibitor Nogo-A establishes spatial segregation and extent of oligodendrocyte myelination. Proc. Natl. Acad. Sci. USA. 2012; 109:1299–1304. [PubMed: 22160722]

Czopka T, Lyons DA. Dissecting mechanisms of myelinated axon formation using zebrafish. Methods Cell Biol. 2011; 105:25–62. [PubMed: 21951525]

Dawson MRL, Polito A, Levine JM, Reynolds R. NG2-expressing glial progenitor cells: an abundant and widespread population of cycling cells in the adult rat CNS. Mol. Cell. Neurosci. 2003; 24:476–488. [PubMed: 14572468]

Fields RD. Neuroscience. Change in the brain's white matter. Science. 2010; 330:768–769. [PubMed: 21051624]

Franklin RJM. Why does remyelination fail in multiple sclerosis? Nat. Rev. Neurosci. 2002; 3:705–714.

Franklin RJ, ffrench-Constant C. Remyelination in the CNS: from biology to therapy. Nat. Rev. Neurosci. 2008; 9:839–855. [PubMed: 18931697]

Europe PMC Funders Author Manuscripts

Europe PMC Funders Author Manuscripts

Fünfschilling U, Supplie LM, Mahad D, Boretius S, Saab AS, Edgar J, Brinkmann BG, Kassmann CM, Tzvetanova ID, Möbius W, et al. Glycolytic oligodendrocytes maintain myelin and long-term axonal integrity. Nature. 2012; 485:517–521. [PubMed: 22622581]

Jopling C, den Hertog J. Fyn/Yes and non-canonical Wnt signalling converge on RhoA in vertebrate gastrulation cell movements. EMBO Rep. 2005; 6:426–431. [PubMed: 15815683]

Kang SH, Fukaya M, Yang JK, Rothstein JD, Bergles DE. NG2+ CNS glial progenitors remain committed to the oligodendro cyte lineage in postnatal life and following neurodegeneration. Neuron. 2010; 68:668–681. [PubMed: 21092857]

Kirby BB, Takada N, Latimer AJ, Shin J, Carney TJ, Kelsh RN, Appel B. In vivo time-lapse imaging shows dynamic oligodendrocyte progenitor behavior during zebrafish development. Nat. Neurosci. 2006; 9:1506–1511. [PubMed: 17099706]

Krämer-Albers E-M, White R. From axon-glial signalling to myelination: the integrating role of oligodendroglial Fyn kinase. Cell. Mol. Life Sci. 2011; 68:2003–2012. [PubMed: 21207100]

Kwan KM, Fujimoto E, Grabher C, Mangum BD, Hardy ME, Campbell DS, Parant JM, Yost HJ, Kanki JP, Chien CB. The Tol2kit: a multisite gateway-based construction kit for Tol2 transposon transgenesis constructs. Dev. Dyn. 2007; 236:3088–3099. [PubMed: 17937395]

Lamason RL, Mohideen MA, Mest JR, Wong AC, Norton HL, Aros MC, Jurynec MJ, Mao X, Humphreville VR, Humbert JE, et al. SLC24A5, a putative cation exchanger, affects pigmentation in zebra-fish and humans. Science. 2005; 310:1782–1786. [PubMed: 16357253]

Laursen LS, Chan CW, ffrench-Constant C. An integrin-contactin complex regulates CNS myelination by differential Fyn phosphorylation. J. Neurosci. 2009; 29:9174–9185. [PubMed: 19625508]

Lee Y, Morrison BM, Li Y, Lengacher S, Farah MH, Hoffman PN, Liu Y, Tsingalia A, Jin L, Zhang P-W, et al. Oligodendroglia metabolically support axons and contribute to neurodegeneration. Nature. 2012; 487:443–448. [PubMed: 22801498]

Liu J, Dietz K, DeLoyht JM, Pedre X, Kelkar D, Kaur J, Vialou V, Lobo MK, Dietz DM, Nestler EJ, et al. Impaired adult myelination in the prefrontal cortex of socially isolated mice. Nat. Neurosci. 2012; 15:1621–1623. [PubMed: 23143512]

Makinodan M, Rosen KM, Ito S, Corfas G. A critical period for social experience-dependent oligodendrocyte maturation and myelination. Science. 2012; 337:1357–1360. [PubMed: 22984073]

Miller DJ, Duka T, Stimpson CD, Schapiro SJ, Baze WB, McArthur MJ, Fobbs AJ, Sousa AMM, Sestan N, Wildman DE, et al. Prolonged myelination in human neocortical evolution. Proc. Natl. Acad. Sci. USA. 2012; 109:16480–16485. [PubMed: 23012402]

Nave KA. Myelination and support of axonal integrity by glia. Nature. 2010; 468:244–252. [PubMed: 21068833]

Ng AN, de Jong-Curtain TA, Mawdsley DJ, White SJ, Shin J, Appel B, Dong PD, Stainier DY, Heath JK. Formation of the digestive system in zebrafish: III. Intestinal epithelium morphogenesis. Dev. Biol. 2005; 286:114–135. [PubMed: 16125164]

Park HC, Shin J, Roberts RK, Appel B. An olig2 reporter gene marks oligodendrocyte precursors in the postembryonic spinal cord of zebra-fish. Dev. Dyn. 2007; 236:3402–3407. [PubMed: 17969181]

Provost E, Rhee J, Leach SD. Viral 2A peptides allow expression of multiple proteins from a single ORF in transgenic zebrafish embryos. Genesis. 2007; 45:625–629. [PubMed: 17941043]

Remahl S, Hildebrand C. Relations between axons and oligodendroglial cells during initial myelination. II. The individual axon. J. Neurocytol. 1990; 19:883–898. [PubMed: 2292718]

Richardson WD, Young KM, Tripathi RB, McKenzie I. NG2-glia as multipotent neural stem cells: fact or fantasy? Neuron. 2011; 70:661–673. [PubMed: 21609823]

Savas JN, Toyama BH, Xu T, Yates JR 3rd, Hetzer MW. Extremely long-lived nuclear pore proteins in the rat brain. Science. 2012; 335:942. [PubMed: 22300851]

Sherman DL, Brophy PJ. Mechanisms of axon ensheathment and myelin growth. Nat. Rev. Neurosci. 2005; 6:683–690. [PubMed: 16136172]

Umemori H, Sato S, Yagi T, Aizawa S, Yamamoto T. Initial events of myelination involve Fyn tyrosine kinase signalling. Nature. 1994; 367:572–576. [PubMed: 7509042]

Wake H, Lee PR, Fields RD. Control of local protein synthesis and initial events in myelination by action potentials. Science. 2011; 333:1647–1651. [PubMed: 21817014]

Watkins TA, Emery B, Mulinyawe S, Barres BA. Distinct stages of myelination regulated by gamma-secretase and astrocytes in a rapidly myelinating CNS coculture system. Neuron. 2008; 60:555–569. [PubMed: 19038214]

White RM, Sessa A, Burke C, Bowman T, LeBlanc J, Ceol C, Bourque C, Dovey M, Goessling W, Burns CE, Zon LI. Transparent adult zebrafish as a tool for in vivo transplantation analysis. Cell Stem Cell. 2008; 2:183–189. [PubMed: 18371439]

Young KM, Psachoulia K, Tripathi RB, Dunn S-J, Cossell L, Attwell D, Tohyama K, Richardson WD. Oligodendrocyte dynamics in the healthy adult CNS: evidence for myelin remodeling. Neuron. 2013; 77:873–885. [PubMed: 23473318]

Zatorre RJ, Fields RD, Johansen-Berg H. Plasticity in gray and white: neuroimaging changes in brain structure during learning. Nat. Neurosci. 2012; 15:528–536. [PubMed: 22426254]

Zawadzka M, Rivers LE, Fancy SPJ, Zhao C, Tripathi R, Jamen F, Young K, Goncharevich A, Pohl H, Rizzi M, et al. CNS-resident glial progenitor/stem cells produce Schwann cells as well as oligodendrocytes during repair of CNS demyelination. Cell Stem Cell. 2010; 6:578–590. [PubMed: 20569695]

Europe PMC Funders Author Manuscripts

Europe PMC Funders Author Manuscripts

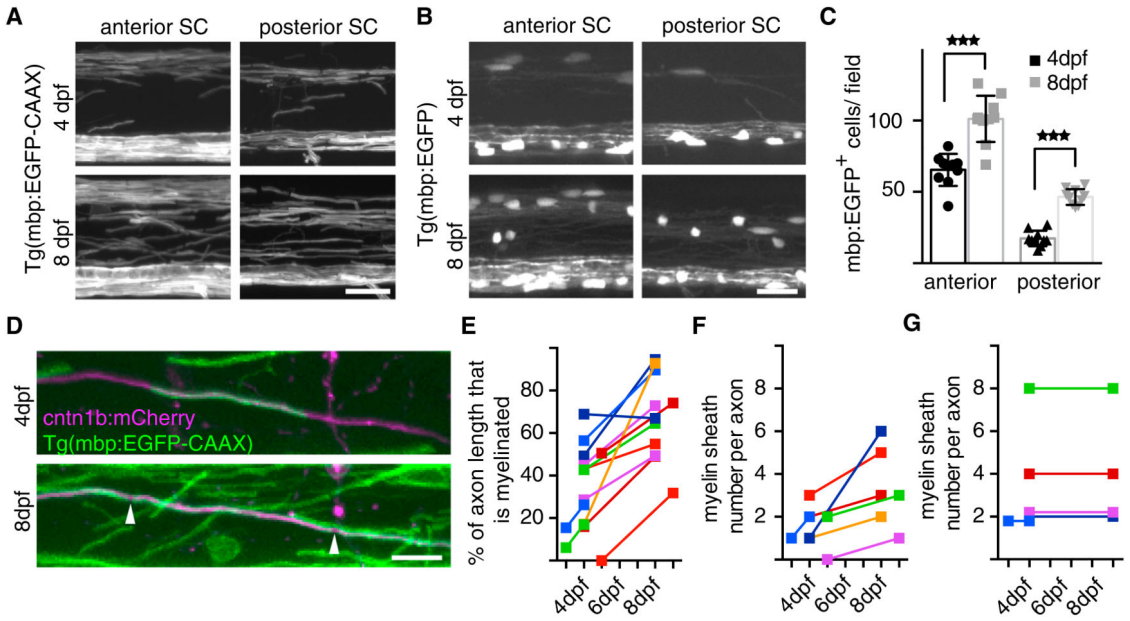


**Figure 1. Dynamic Change in Global Myelination in the Larval Zebrafish Spinal Cord**

(A) Lateral views of the anterior (left) and posterior (right) spinal cord in Tg(mbp:EGFP-CAAX) animals at 4 days postfertilization (dpf) (top) and 8 dpf (bottom) indicate a significant increase in the number of myelin sheaths over this period. Scale bar, 20 μm.

(B) Lateral views of the anterior (left) and posterior (right) spinal cord in Tg(mbp:EGFP) animals at 4 days postfertilization (dpf) (top) and 8 dpf (bottom) indicate a significant increase in the number of myelinating oligodendrocytes over this period. Scale bar, 20 μm.

(C) Quantification of myelinating oligodendrocyte number in the anterior and posterior spinal cord at 4 and 8 dpf. Significance was tested using Student's two-tailed unpaired t test. Error bars indicate SD.

(D) Lateral views of a single axon labeled by cntn1b:mCherry and myelin sheaths labeled with Tg(mbp:EGFP-CAAX) at 4 dpf (top) and 8 dpf (bottom) show that the deposition of new myelin sheaths along single axons can occur over the course of several days. Arrowheads indicate putative nodes of Ranvier. Scale bar, 10 μm.

(E) Quantification of the percentage axon length covered by myelin between 4 and 9 dpf. Each line represents a distinct axon.

(F) Subset of axons shown in (E) where myelin sheath number increased over time.

(G) Subset of axons shown in (E) where myelin sheath number does not change over time.



Europe PMC Funders Author Manuscripts
Europe PMC Funders Author Manuscripts

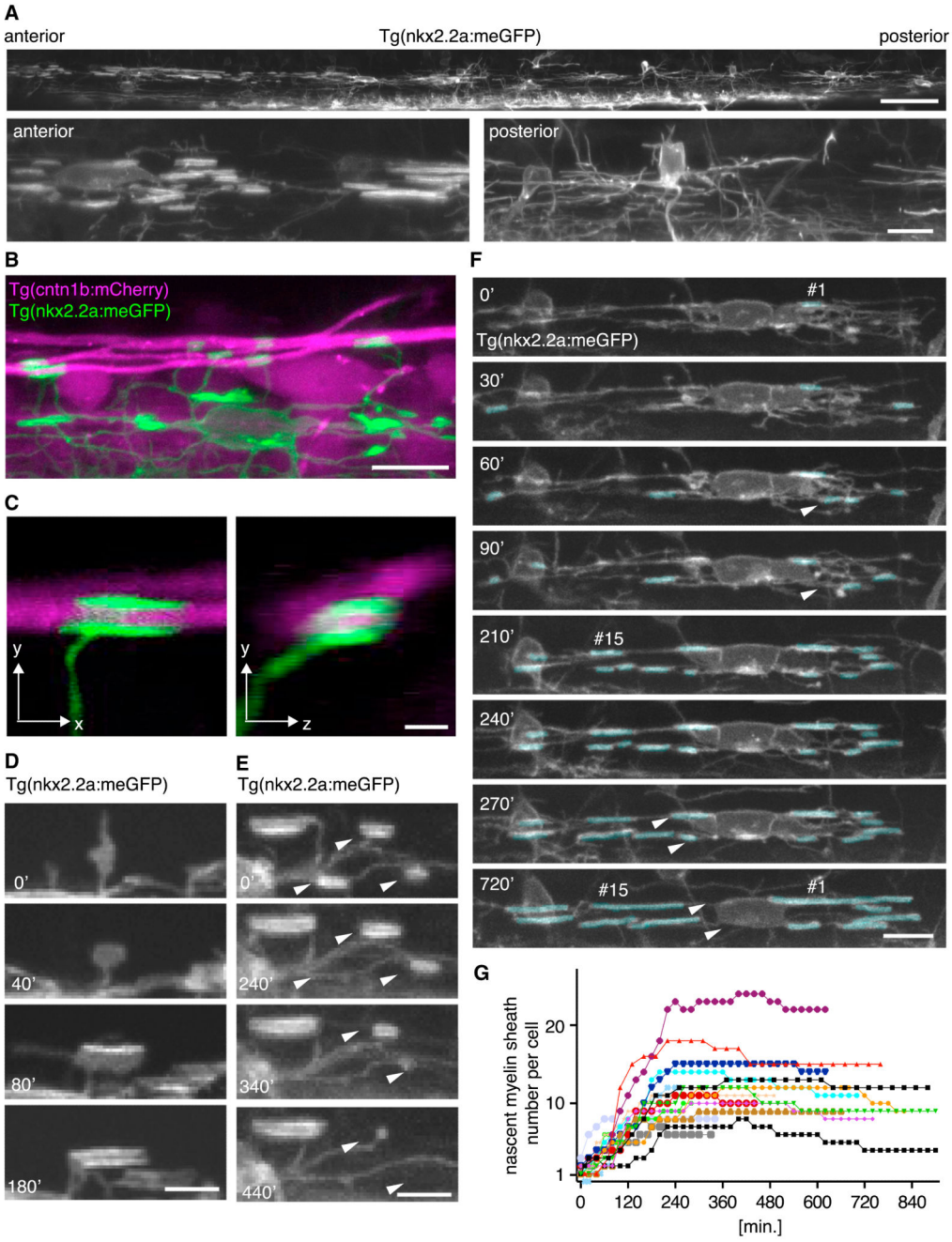


**Figure 2. Individual Oligodendrocytes Initiate New Myelin Sheaths in a Short Time Window**

(A) Top: lateral view of a 0.75 mm stretch of the zebrafish spinal cord at 3 dpf indicates a gradient from anterior to posterior in the differentiation status of oligodendrocytes in a Tg(nkx2.2a:meGFP) animal. Scale bar, 50 μm. Bottom: cells located in the anterior spinal cord have a mature myelinating morphology (left), whereas those in more posterior regions of the spinal cord have a less mature premyelinating morphology (right). Scale bar, 10 μm.

(B) Lateral view of a Tg(nkx2.2a:mEGFP), Tg(cntn1b:mCherry) double transgenic zebrafish at 3 dpf shows a single oligodendrocyte with nascent myelin sheaths surrounding axons. Scale bar, 10 μm.



Europe PMC Funders Author Manuscripts
Europe PMC Funders Author Manuscripts

(C) Higher magnification x,y (left panel) and x,z (right panel) views of a Tg(nkx2.2a:mEGFP), Tg(cntn1b:mCherry) animal confirm that nkx2.2a:mEGFP-labeled oligodendrocyte processes surround axons. Scale bar, 2 μm.

(D) Single selected images from a time-lapse series of an oligodendrocyte process in a Tg(nkx2.2a:mEGFP) zebrafish reveal transformation of an exploratory process into a myelin sheath within a few hours. Scale bar, 5 μm.

(E) Single selected images from a time-lapse series showing that nascent myelin sheaths can be retracted (arrowheads) over a period of a few hours. Scale bar, 5 μm.

(F) Selected images from a time-lapse series of a single oligodendrocyte in a Tg(nkx2.2a:mEGFP) animal. The cell makes its first nascent myelin sheath (indicated by “#1”) at time point zero (see main text) and its final new myelin sheath (indicated by “#15”) by the 210 min time point. Examples of nascent myelin sheaths that are retracted during the time-lapse are indicated by arrowheads. Scale bar, 10 μm.

(G) Total number of nascent myelin sheaths for 16 different oligodendrocytes over time. Time point zero is the time at which each oligodendrocyte initiates its first myelin sheath. The cell from (F) is colored in cyan. See also Movie S1.

Europe PMC Funders Author Manuscripts

Europe PMC Funders Author Manuscripts

Europe PMC Funders Author Manuscripts

Europe PMC Funders Author Manuscripts

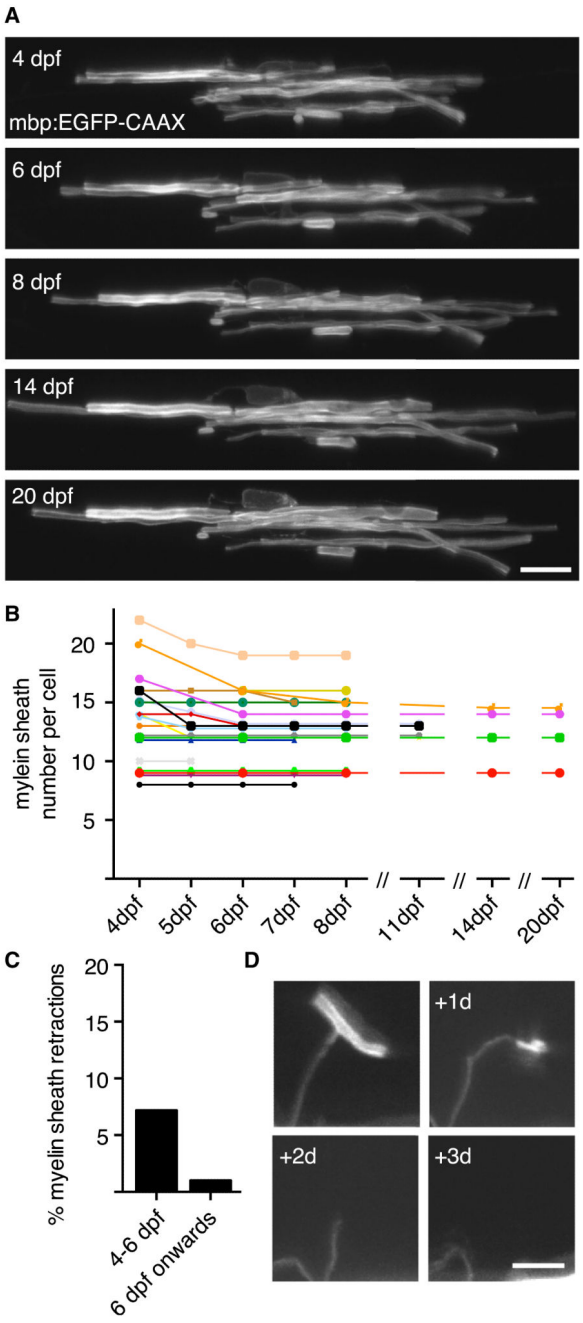


**Figure 3. Mature Myelinating Oligodendrocytes Never Generate New Myelin Sheaths but Do Remove a Small Number over Time**

(A) Single mbp:EGFP-CAAX-expressing oligodendrocyte imaged from 4 through 20 dpf. Scale bar, 10 μm.

(B) Quantification of myelin sheath number of individual myelinating oligodendrocytes over time.

(C) Percentage of myelin sheath retractions over the time periods analyzed in (B).

(D) Confocal images of a single myelinating process at 4 dpf (left) that is retracted slowly over the course of the following 3 days. Scale bar, 5 μm.

See also Figure S3 and Movies S4 and S5.

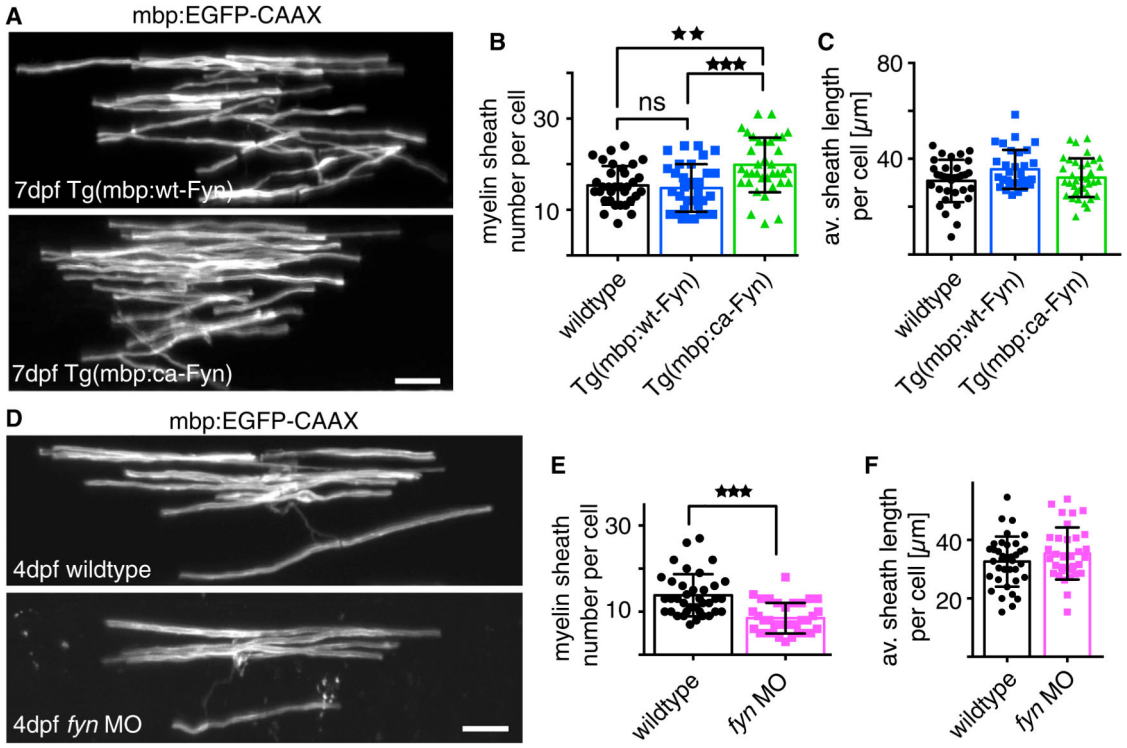


**Figure 4. Manipulation of Fyn Alters Myelin Sheath Number per Oligodendrocyte**

(A) mbp:EGFP-CAAX-expressing oligodendrocytes at 7 dpf in Tg(mbp:wt-Fyn) (top) and Tg(mbp:ca-Fyn) animals (bottom). Scale bar, 10 μm.

(B) Oligodendrocytes in Tg(mbp:ca-Fyn) animals have a higher number of myelin sheaths than control or those in Tg(mbp:wt-Fyn) animals. Significance was assessed using one-way ANOVA. Error bars indicate SD.

(C) The average length of myelin sheath per cell is not significantly different between control, Tg(mbp:wt-Fyn), or Tg(mbp:ca-Fyn) animals. Significance was assessed using one-way ANOVA. Error bars indicate SD.

(D) mbp:EGFP-CAAX-expressing oligodendrocytes in control (top) and *fyn* morphant (bottom). Scale bar, 10 μm.

(E) *fyn* morphants have a reduction in myelin sheath number per cell compared to control. Significance was assessed using Student's two-tailed unpaired t test. Error bars indicate SD.

(F) The average length of myelin sheaths per cell does not change following Fyn loss-of-function. Significance was assessed using Student's two-tailed unpaired t test. Error bars indicate SD.

See also Figures S1 and S2.



Europe PMC Funders Author Manuscripts
Europe PMC Funders Author Manuscripts

Europe PMC Funders Author Manuscripts

Europe PMC Funders Author Manuscripts

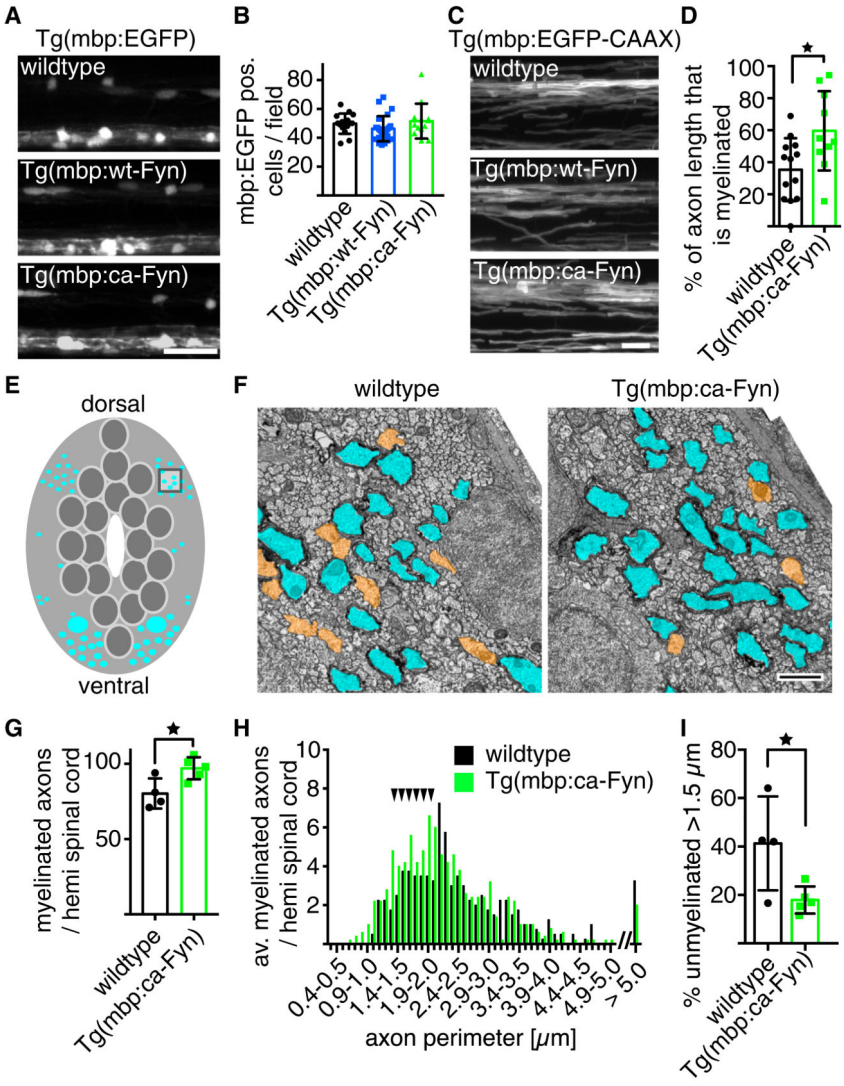


**Figure 5. Constitutive Activation of Fyn in Myelinating Oligodendrocytes Causes Precocious Myelination without Affecting Cell Number**

(A) Confocal images of Tg(mbp:EGFP) wild-type control (top), Tg(mbp:wt-Fyn) (middle), and Tg(mbp:ca-Fyn) (bottom) animals at 8 dpf show no difference in oligodendrocyte number or distribution. Scale bar, 25 μm.

(B) Quantification of myelinating oligodendrocyte number at 8 dpf reveals no differences between wild-type, Tg(mbp:wt-Fyn), and Tg(mbp:ca-Fyn) animals. Significance was assessed using one-way ANOVA. Error bars indicate SD.

(C) High-magnification views of the dorsal spinal cord at 8 dpf in Tg(mbp:EGFP-CAAX) control (top), Tg(mbp: wt-Fyn) (middle), and Tg(mbp:ca-Fyn) (bottom) animals show that there are additional myelinated axons in Tg(mbp:ca-Fyn) animals. Scale bar, 10 μm.

(D) Quantification showing percentage of single axon length myelinated in control compared to Tg(mbp:ca-Fyn) animals by 5 dpf. Significance was assessed using Student's two-tailed unpaired t test. Error bars indicate SD.

(E) Schematic transverse cross-section of the larval zebrafish spinal cord indicating myelinated axons in cyan.

(F) Transmission electron microscope images of transverse sections of spinal cords at 8 dpf of an area indicated in (E) in wild-type (left) and Tg(mbp:ca-Fyn) (right) animals. There is a larger number of myelinated axons (shaded in cyan) in Tg(mbp:ca-

Fyn) animals and a smaller number of large caliber (>1.5mm perimeter) unmyelinated axons (shaded in orange). Scale bar, 1 μm.

(G) The number of myelinated axons per hemi spinal cord is increased in Tg(mbp:ca-Fyn) animals compared to wild-type. Significance was assessed using Student's two-tailed t test. Error bars indicate SD.

(H) The distribution of myelinated axon size (assessed by axonal perimeter) in wild-type and Tg(mbp:ca-Fyn) animals is similar. The additional axons myelinated in Tg(mbp:ca-Fyn) animals compared to control are almost all between 1 and 2 μm in perimeter (arrowheads).

(I) Quantification of percentage unmyelinated axons with a perimeter >1.5 μm in wild-type and Tg(mbp:ca-Fyn) dorsal spinal cord. Significance was assessed using Student's two-tailed unpaired t test. Error bars indicate SD.

See also Figure S1.

Europe PMC Funders Author Manuscripts

Europe PMC Funders Author Manuscripts

Europe PMC Funders Author Manuscripts

Europe PMC Funders Author Manuscripts

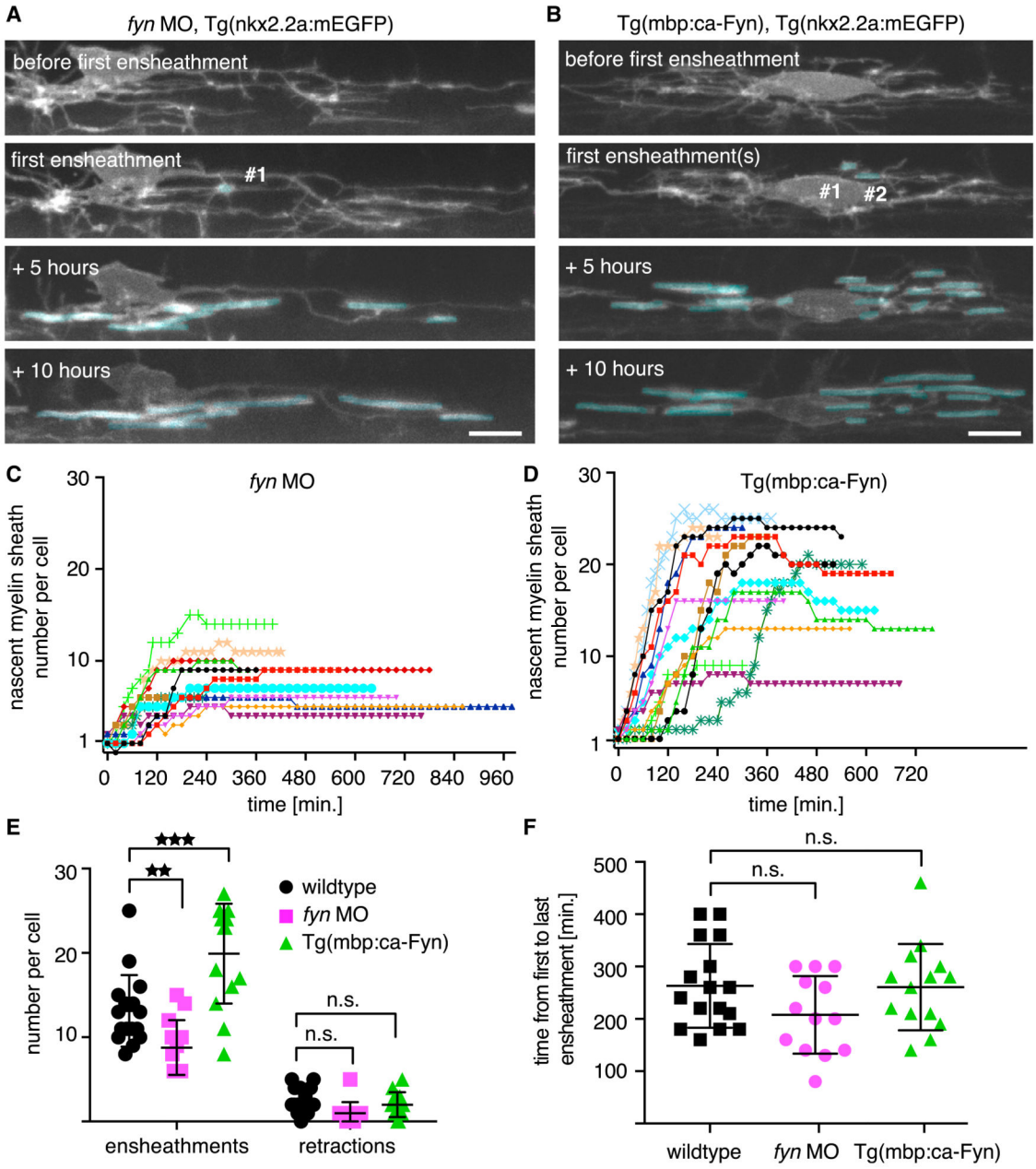


**Figure 6. Myelin Sheaths Are Generated during the Same Short Dynamic Period following Fyn Loss and Gain of Function**

(A) Images of a single oligodendrocyte in a Tg(nkx2.2a:mEGFP) *fyn* morphant during initiation of myelination. The first ensheathment is indicated with "#1." Scale bar, 10 μm.

(B) Images of a single oligodendrocyte in a Tg(nkx2.2a:mEGFP), Tg(mbp:ca-Fyn) animal during initiation of myelination. The first ensheathments are indicated with "#1" and "#2." Scale bar, 10 μm.

(C) Total number of nascent myelin sheaths for 13 different *fyn* morphant oligodendrocytes over time. Time point zero is set as the time at which each oligodendrocyte starts to make its first myelin sheath. The cell from (A) is colored in cyan.

(D) Total number of nascent myelin sheaths for 14 different oligodendrocytes in Tg(mbp:ca-Fyn) animals over time. Time-point zero is set as the time at which each oligodendrocyte starts to make its first myelin sheath. The cell from (B) is colored in cyan.

(E) Ensheathment, but not retraction, number changes with Fyn manipulation. Significance was assessed using two-way ANOVA. Error bars indicate SD.

(F) The duration of myelin sheath formation by individual oligodendrocytes is similar in wild-type, *fyn* morphant, and Tg(mbp:ca-Fyn) animals. Significance was assessed using one-way ANOVA. Error bars indicate SD.

See also Figures S1 and S2 and Movies S1, S2, and S3.

Europe PMC Funders Author Manuscripts

Europe PMC Funders Author Manuscripts